

**FEDSM-ICNMM2010-3051**

## **ORGANIZATION OF CYLINDER WAKE USING A SPLITTER-PLATE ACTIVE FLOW CONTROL**

**Chris Weiland**

Virginia Tech Department of Mechanical  
Engineering

**Pavlos Vlachos**

Virginia Tech Department of Mechanical  
Engineering

### **ABSTRACT**

Time Resolved Digital Particle Image Velocimetry (TRDPIV) was used in conjunction with spectral analysis to study the effects of Leading Edge Blowing (LEB) flow control on the near-wake of a circular cylinder. The airfoil was placed 1.9 circular cylinder diameters downstream, effectively acting as a splitter plate. Spectral measurements of the TRDPIV results indicated that the presence of the airfoil decreased the Strouhal number from 0.19 to 0.12 as anticipated.

When activated the LEB jet organized the circular cylinder wake, effectively neutralizing the effect of the splitter plate and modifying the wake so as to return the Strouhal number to 0.19. Thus the circular cylinder wake returned to its normal shedding frequency, even in the presence of the airfoil. Evidence presented in this study supports the notion that the LEB jet directly excites the circular cylinder shear layers causing instability, roll up, and subsequent vortex shedding.

### **INTRODUCTION**

The interaction of an airfoil with incident vortices or wakes has received great attention over the years. These phenomena are of practical significance for engineering applications as it is commonly encountered in fluid-structure interactions and the resulting fluctuating loads exerted on a structure can contribute to detrimental effects, fatigue or even catastrophic failure ([1]; [2]). Many studies have focused on the far-wake interaction between airfoils and vortices, examples of which are the excitation of a helicopter blade due to an upstream rotor wake [3] or the vibration of the rotor due to the inlet guide vane wake commonly found in turbomachinery ([4]; [5]). For the purpose of reducing the unsteady loading on helicopter blades, a multitude of strategies have been proposed to mitigate the unsteady loading of the airfoil as a result of this blade vortex interaction (BVI). These strategies include methods for increasing the stand-off distance between a vortex and the

airfoil [6], flow control to decrease the strength of the incident vortices [7], or airfoil surface modifications such as porous leading edge surfaces which have been shown to reduce the radiated pressure field [8]. Recent work by the authors reported on a flow control scheme based on Leading Edge Blowing (LEB) that successfully reduced the transfer of energy from an unsteady vortical flow field to an airfoil [9]. The LEB jet was able to reduce airfoil vibrations by creating a virtual leading edge upstream of the physical leading edge displacing the upcoming vortices further from the airfoil surface and resulting in a 38% reduction of induced vibrations based on the root-mean-square of the airfoil velocity oscillation amplitude. In these experiments, the airfoil leading edge was located 5.8 diameters downstream of the vortex generator and thus constituted a far-field BVI.

Herein we extend the previous study by focusing on the near-field interaction between the airfoil, the circular cylinder wake and the LEB jet. Experiments were conducted with the airfoil leading edge located at 1.9 diameters downstream of the circular cylinder. Therefore the airfoil is within the mean closure point of the wake and can behave almost like a splitter plate disruption the wake of the circular cylinder. Splitter plates mounted to a cylinder have been largely researched as a passive mechanism to reduce base drag [10], suppress shedding in the wake of the circular cylinder [11], control noise due to circular cylinder shedding ([12]; [13]), and as a means to study the circular cylinder vortex shedding processes ([14]; [15]). Current understanding suggests that the interaction of the cylinder shear layers is a fundamental process that contributes to the absolute instability in the wake and controls the shedding process. Lin et al [16] and Unal and Rockwell [17] have also considered the effects of convective instability on the shedding process.

The effect of splitter plates on suppression of the vortex street has been well documented. Grove et al [18] studied the

effect of splitter plates of length  $2D$  to  $4D$  (where  $D$  is the circular cylinder diameter) and found their effect to be a maximum when the near side of the splitter plate was located  $2D$  to  $3D$  downstream of the circular cylinder. The experiments of Unal and Rockwell [19] suggest a minimum length scale for the development of the absolute instability and subsequent vortex formation. Additionally, they note that the vortex formation process is possibly influenced by the vorticity dynamics downstream, such as could be caused by impingement of vortices on the airfoil. This type of interaction has been well studied ([20]; [21]). However, the focus of this paper is on the effect of LEB flow control on the near-wake structure and little attention is paid to possible feedback mechanisms through vortex impingement on the airfoil.

The idea of downstream disturbances affecting the vortex formation process is particularly relevant to the current study because the turbulent planar jet used for LEB has been shown to display rich physics such as coherent structures ([22]; [23]) which closely resembles that of a von Karman vortex street. Additionally, strong interactions exist between these structures within the plane jet, which are thought to give rise to the familiar flapping mode often observed [24]. In this paper we will show that the interaction of the planar jet and the circular cylinder wake has significant effect on the organization of the wake and can reverse the ability of the splitter plate to modify the near wake structure.

Since the airfoil is close to the circular cylinder, it is also possible that the LEB jet could strike the lee side of the circular cylinder and contribute to the global instability of the system. Jet impingement on circular cylinders has been studied in the past for both plane ([25]; [26]) and round ([27]; [28]; [29]) jets; however these studies have been limited to jets impinging on a circular cylinder or convex/concave surfaces in quiescent flow. These studies revealed feedback mechanisms that exist between the jet and circular cylinder wake instabilities [25] through the upstream amplification of perturbations that act on the jet due to impingement. The contribution of this feedback mechanism to the cylinder shedding process has not been explored. In the case of a round jet impinging on a flat plate (i.e. without curvature effects), it was found that the toroidal vortex structures formed from the jet shear layer impact the flat plate, where they are effectively stretched before they are absorbed and dispersed in the turbulent radial wall jet [27]. Based on these past studies of jet/circular cylinder impingement under quiescent conditions one can assert that a boundary layer induced on the back surface of the circular cylinder by the LEB could perturb the separating boundary layer and the resulting shear layers, therefore influencing the vortex formation and shedding mechanisms. However, in all of the above past studies there was no cross flow, and thus the effect of the circular cylinder boundary layer, the vortices shed from the cylinder, and their interaction with the jet shear layer were not considered.

The present study is concerned with identifying the interaction mechanism between the LEB jet, the airfoil (which acted as a splitter plate), and the circular cylinder wake. Although the data presented here are a subset of a more extensive parametric study on the effects of LEB on BVI mitigation, herein we focus on those cases associated with the amplification of BVI through the LEB jet/circular cylinder wake interaction. The interaction was experimentally studied using Time Resolved Digital Particle Image Velocimetry (TRDPIV) and subsequently the velocity fields were analyzed using both spectral analyses and Proper Orthogonal Decomposition (POD). The airfoil motion was recorded using simultaneous accelerometer measurements. The LEB jet was found to exert a sizable influence on the near wake structure of the circular cylinder, effectively organizing the near wake so as to generate a shedding mode similar to the 2P mode defined by Williamson (1996). Organization of the near wake neutralized the effects of the airfoil, which acted as a splitter plate, and the Strouhal number was returned to its nominal value resulting in increased airfoil vibrations.

## NOMENCLATURE

$U$	Velocity
$M$	Flow Control Momentum Coefficient
$c$	Airfoil Chord Length
$D$	Cylinder Diameter
$f$	Cylinder Shedding Frequency
$w$	Airfoil Thickness at Mid-Chord
$h$	Flow Control Jet Slot Height
$v$	Component of Velocity Normal to Freestream
$x$	Position Parallel to Airfoil Chord
$y$	Position Orthogonal to Airfoil Chord
$\eta$	Airfoil Leading Edge to Circular Cylinder Mount Point
$q$	Airfoil span
$St$	Strouhal number
$\sigma$	Standard deviation

## SUBSCRIPTS

$\infty$	Freestream condition
$j$	LEB jet parameter

## EXPERIMENTAL

The velocity field was characterized using Time Resolved Digital Particle Image Velocimetry (TRDPIV). In addition, the airfoil vibration was also measured using an accelerometer mounted to a strut that was rigidly connected to and vibrated with the airfoil. Experimental setup details may be found in Weiland and Vlachos (2009) but a brief overview of the experimental setup and procedures is also provided here.

The experiments were conducted in the water tunnel in the Virginia Tech, Department of Engineering Sciences and Mechanics, Fluid Mechanics Laboratory. The water tunnel is able to produce a low-turbulence (3%) freestream of up to 1 m/s within a test section of 0.6x0.6x1.5m. A sharp leading and

trailing edge airfoil with a chord of 0.097m and span of 0.2m was placed downstream and parallel to a circular cylinder at zero degrees angle of attack along the centerline of the circular cylinder. The airfoil is a symmetric double arc, with a maximum thickness of 0.015m. A leading edge slot, used for the injection of the jet, extends almost the entire span of the airfoil and is located at its bottom side only. The jet is issued in a direction aligned with the free stream.

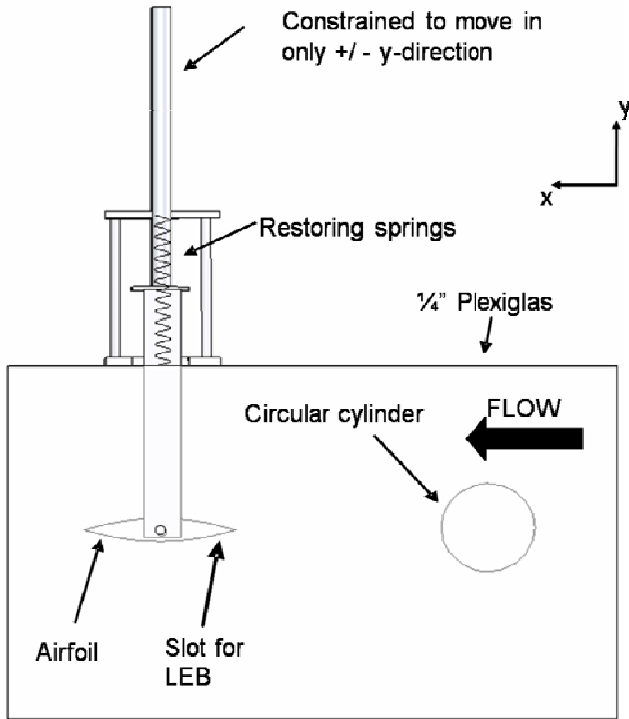


**Figure 1. Side view of the test apparatus. The airfoil is rigidly mounted to a strut constrained to move in the y-direction only. The circular cylinder is rigidly mounted to two parallel acrylic plates used as end-walls.**

The airfoil was allowed to oscillate in response to the wake of the cylinder, and linear springs restored the airfoil to its rest position. The airfoil was constrained to only move in a direction perpendicular to the flow direction by two rods on linear bearings rigidly mounted to the airfoil outside of the test section. Two accelerometers (Wilcoxon Research, model 752-3, sensitivity of +/- 10%) were attached to a strut rigidly mounted to the airfoil and recorded the vibration velocity signal in time. Plexiglas side-walls contained the airfoil and the circular cylinder in the (x,y) plane in order to permit optical access but provide symmetric end-conditions and limit three dimensional effects, such as wing tip vortices and shedding from the circular cylinder free-end. The Plexiglas walls were 6.35mm thick mounted on 3.17mm thick angle steel for structural integrity. The end-walls' dimensions were 0.6m (flow direction) x 0.3m (normal to flow). This allowed about 0.2m of end-wall upstream of the circular cylinder mount point and 0.12m downstream of the airfoil. All struts and mount points were located outside of the Plexiglas sheet. The system

(i.e. the arrangement of Figure 1 in the presence of water with no cross flow) was rigidly mounted in the test section and its natural frequency was experimentally determined to be 12 Hz by impulsively impacting the airfoil strut and measuring the response of the accelerometers. Several springs were tested to find the optimal spring stiffness, since a trade-off occurs between accelerometer sensitivity and the structural resonance frequency of the system. If a stiff spring is chosen to move the system natural frequency away from the shedding frequency of the circular cylinder, the airfoil will not move in response to the wake and the accelerometer cannot resolve this signal. The spring stiffness was specifically chosen to move the natural frequency of the system away from the circular cylinder shedding frequency to avoid any structural resonance effects while still giving a good signal-to-noise ratio in the accelerometer measurements.

The freestream velocity was kept constant at 0.55 m/s giving a Reynolds number of 27940 based on circular cylinder diameter. The circular cylinder was mounted 0.12m upstream of the airfoil tip (1.9 diameters). Thus the airfoil is exactly within the range specified by Grove et al [18] for being the best possible location for suppression of the vortex street. The circular cylinder shedding frequency was calculated using the Strouhal relationship, shown in Equation 1. Here the Strouhal number,  $St$ , is given by the empirical relationship presented by Fey et al [30] and for the circular cylinder Reynolds number used here, it was estimated to be approximately  $St=0.191$ .

$$f_s = \frac{StU_\infty}{D} \quad (1)$$

For the purpose of flow control, water was fed into the airfoil by two 1/4 inch tubes on either side of the airfoil via two electronically controlled positive displacement pumps (Ismatec model BVP-Z) working in parallel. The flow rate was recorded using an ultrasonic flow meter (Transonic Systems Inc., model T110). The flowmeter was calibrated in-house yielding an accuracy of 15%. The airfoil has a blowing slot on its leading edge located on the bottom side of the airfoil with the jet axis aligned with the free stream. The plane jet was issued at an aspect ratio ( $q/h$ ) of 127. The momentum coefficient of the jet,  $M$ , is defined in Equation 2. Only steady jets and two blowing conditions, no blowing and  $M=0.105$ , were considered in this study.

$$M = \frac{U_j^2 h}{U_\infty^2 t} \quad (2)$$

The jet was characterized in both the spanwise and streamwise directions (at mid-span) using DPIV measurements (the TRDPIV system details are presented in the next section). Results indicate that along the span, the jet profile is nearly Gaussian with the velocity approximately 90% of the mid-span velocity at +/- 5 slot heights (1.5 cm), and 80% of the mid-span velocity at +/- 10 slot heights (3.2 cm). The planar jet growth

normal to the spanwise direction is typical of a planar self-similar jet. These profiles show that the LEB jet is primarily focused in the mid-span section of the airfoil where the DPIV interrogation captures the most dominant interaction. However, this also shows that the jet-wake interaction will be strongly three-dimensional. Further details may be found in Weiland and Vlachos (2009).

**Time Resolved Digital Particle Image Velocimetry Measurements**

Digital Particle Image Velocimetry allows optical, non-invasive, instantaneous point measurements of all velocity components in an interrogation region and has become the most popular experimental fluid mechanics method [31]. Small, neutrally buoyant tracer particles seed the fluid and are illuminated using a planar light sheet. The motion of the particles is captured via digital cameras. The velocity of the particle patterns is estimated using standard digital cross-correlation [32]. Post processing of the data allows calculation of other flow variables, such as vorticity and shear stress.

In this experiment the flow field was illuminated with a Lee Lasers 45W Nd:YAG laser. The laser sheet was delivered from below the airfoil through a Plexiglas window on the bottom side of the water tunnel. The flow was seeded with 11 micron neutrally buoyant spherical hollow glass particles with a specific gravity of 1.1, manufactured by Potters Industries. Motion of the particles was tracked with an IDT XS-3 high-speed camera capable of a maximum resolution of 1280x1024 pixels. The images were processed using in-house developed TRDPIV software utilizing a standard cross-correlation technique. The iterative multigrid DPIV algorithm with discrete window offset was [33] used with two passes of 32x32 pixel and 16x16 pixel interrogation windows respectively with subpixel accuracy of approximately 0.1 pixels. The vector grid spacing was uniform at 8 pixels. The data were validated first using a median filter to remove significantly bad vectors and then an iterative adaptive validation was performed using a mean and standard deviation estimator. The TRDPIV measurements were taken for approximately 4.25 seconds at 800 Hz sampling rate. The interrogation region for the TRDPIV measurements was 1280 pixels by 964 pixels with a resolution of 141 μm/pixel. As the shedding frequency was about 2.1 Hz approximately 9 shedding cycles were captured with a total number of 18369 velocity vectors (1.15mm vector spacing or 0.01D) to resolve the flow field.

Two TRDPIV interrogation regions were chosen and are shown in Figure 2. The first interrogation plane (dotted lines) contains the whole airfoil and a downstream portion of the cylinder wake but not the cylinder. The second plane (solid lines) captures the flow field over approximately 31% of the leeward side of the circular cylinder and extends to approximately the airfoil mid-chord. The downstream distance between the airfoil leading edge and the circular cylinder aft-

end was 0.97 chords or about 1.9 circular cylinder diameters, and the height of the interrogation planes was 1.4 chords.

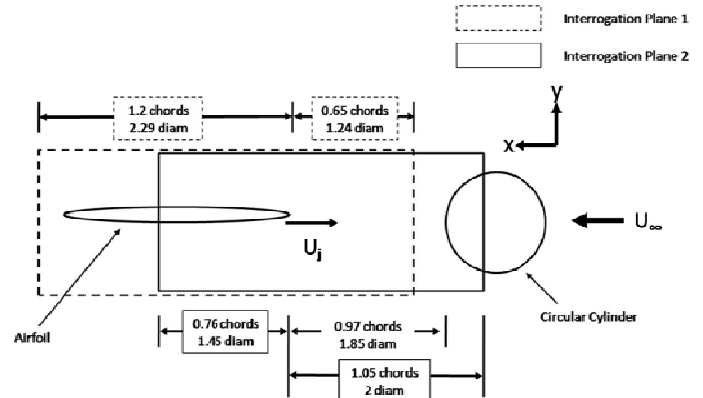


**Figure 2. Field of view used in DPIV experiments. Interrogation plane 1 contained the entire airfoil while interrogation plane 2 contained both airfoil and circular cylinder. Note LEB jet issues in a direction opposite to that of the free stream.**

**Spectral Analysis of the TRDPIV Flow Fields**

Mean-subtracted time-series of point velocity measurements in the flow field and accelerometer time-series were analyzed using a Power Spectrum Density (PSD) routine in Matlab ©. This analysis allowed for characterizing the spectral content of the flow field and performing a comparison of the forcing frequencies by comparing with the simultaneous measurements of the airfoil vibrations. The PSD was computed using a Hamming window with frequency resolution of ½ Hz and 90% overlap between windows was used. The PSD of the v-component velocity fluctuations was estimated spatially across the points in the domain. The PSD of each point along a line drawn transverse to the flow gives a slice of the spectral characteristics of the flow field at different streamwise stations as shown in Figure 3.

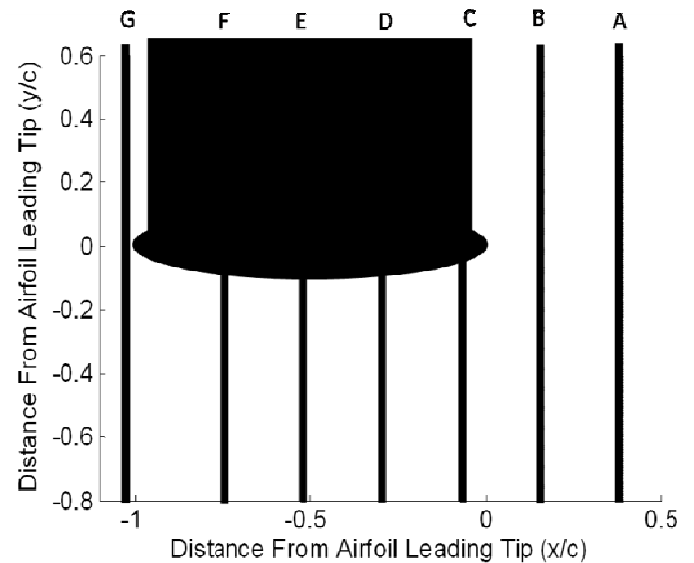


**Figure 3. Flow field spectra were computed at all points along slices of the flow field, thus yielding the distribution of spectral energy at discrete points in the flow. Stations A, B, C, D, E, F, and G correspond to distances of 0.63, 0.40, 0.16, -0.07, -0.30, -0.54, -0.77, and -1.06 chords from the airfoil leading edge.**

## RESULTS AND DISCUSSION

In the following sections we describe results observed and computed for two blowing cases corresponding to  $M=0$  and  $M=0.105$ . Analysis of the airfoil accelerometer time series is presented as it provides an integral view of the effect of LEB on the vortex induced vibration and indirectly demonstrates the degree of the organization of the cylinder wake. Since the airfoil leading edge was located only 1.9 diameters downstream of the circular cylinder, the vortex street did not have enough distance to form therefore the airfoil behaved as a splitter plate with length about  $2D$ . Conversely, the application of LEB increased airfoil oscillations (based on the RMS of the airfoil velocity time history) by about 23% as shown in the PSD analysis of the accelerometer response in Figure 4. For  $M=0.105$  the spectral energy rises sharply around  $f/f_s = 0.9$ . A significant change in the airfoil spectrum is seen over the range  $1 < f/f_s < 6$ . A comparison of the power contained in both cases over the range  $0 < f/f_s < 6$  yields an increase of about 70% for the blowing case.

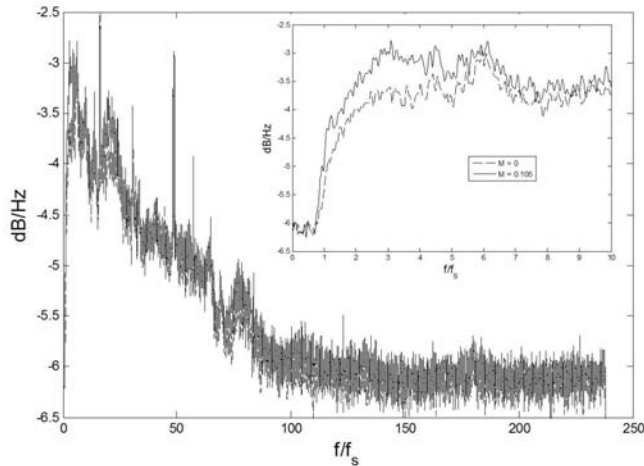


**Figure 4. PSD of the accelerometer data showing a comparison of the response of the airfoil between the no-blowing and LEB cases.**

The airfoil sustained a broad increase in vibration energy for  $M=0.105$  near  $f/f_s = 1$ , indicating the circular cylinder regained its normal shedding frequency. This spectral

component was seen to a much lesser extent in the  $M=0$  case. As past studies have shown ([34]; [17]) splitter plates located in the same region as the airfoil in this experiment have only suppressed circular cylinder shedding or modified the Strouhal number, it is likely that the LEB jet is directly responsible for this change through some mechanism which will be discussed in later sections.

### **Spectral Analysis of the TRDPIV Flow Fields and Evidence of Wake Organization**

PSD plots of the spectral content of the vertical velocity component spatially resolved along different streamwise stations within the first interrogation plane are shown in Figure 5 and Figure 6, for  $M=0$  and  $M=0.105$  respectively. The plotted spectra are zoomed-in around the circular cylinder shedding frequency. Stations A, B, C, D, E, F, and G correspond to distances of 0.63, 0.40, 0.16, -0.07, -0.30, -0.54, -0.77, and -1.06 chords from the airfoil leading edge. The airfoil location is marked with a solid horizontal line. For the case of  $M=0$ , the flow field is relatively free of strong velocity fluctuations in subplot A. In subplots B-E a weak spectral component is seen at or near the circular cylinder shedding frequency ( $f/f_s=1$ ). The strongest frequency component occurs at about  $f/f_s=0.61$  which implies a change of the Strouhal number to 0.12. This is similar to the results reported by Ozono [34], who showed that when the splitter plate was 2 diameters downstream of the circular cylinder they estimated  $St=0.13$ . The weak spectral content at the shedding frequency is explained by the fact that the airfoil acts as a splitter plate. Thus the airfoil is buffeted by gusts of turbulence over a broad range of frequencies as can be seen in the figure for  $M=0$ . For  $M=0.105$  however there are strong spectral components at the shedding frequency in subplots C-G. This increase in spectral energy when LEB is applied suggests that the LEB jet is affecting the wake flow field. This also explains the large increase in the vibration spectral energy of the airfoil observed in Figure 6 near  $f/f_s=1$ . The LEB excites the instabilities associated with the shear layer roll-up and vortex shedding thus organizing the wake near the shedding frequency. Subsequently this flow field energy is transferred on the airfoil. Strong spectra at  $f/f_s=2$  can also be seen in subplots A-G, and it appears that this frequency dominates the upper side of the airfoil. In subplot G a significant spectral component is also seen at about  $f/f_s=0.61$  on the upper side of the airfoil only. It is possible that the asymmetry of the LEB slot is most likely to cause asymmetries of the flow field downstream.

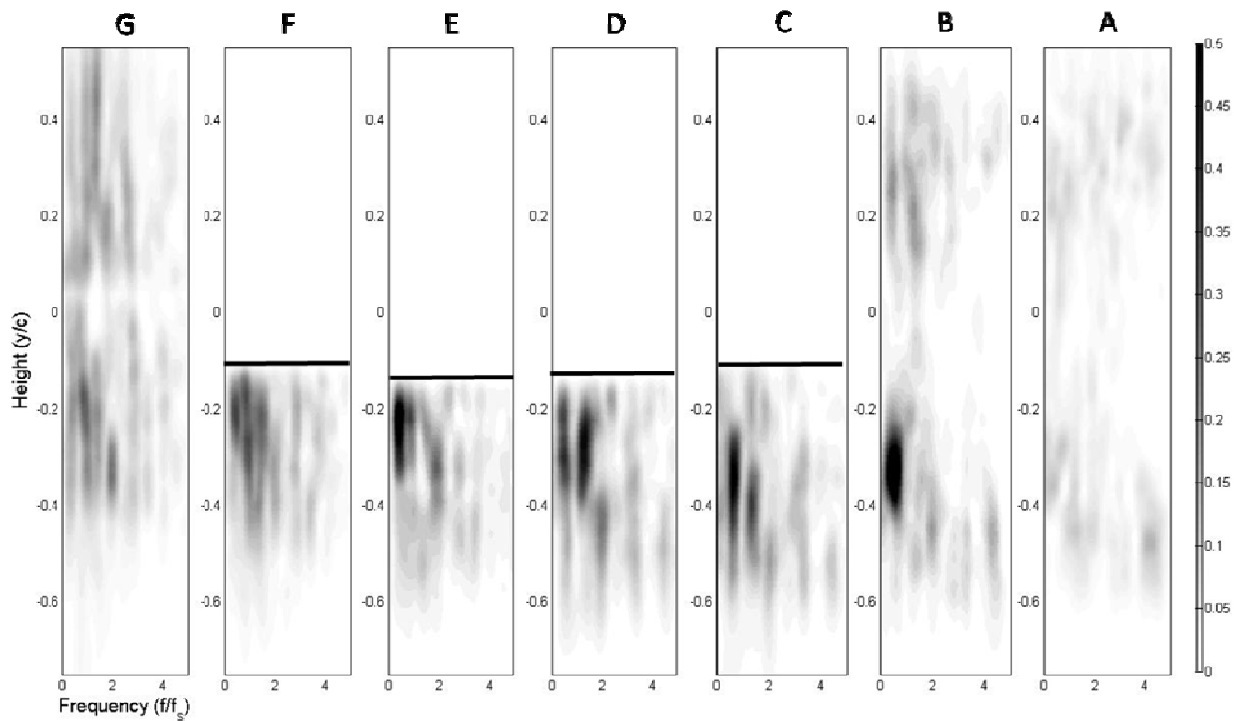


Figure 5. Spectral analysis of DPIV flow field at discrete slices. Airfoil location is noted by black horizontal lines. Note power distributed around, but not at, Strouhal frequency.

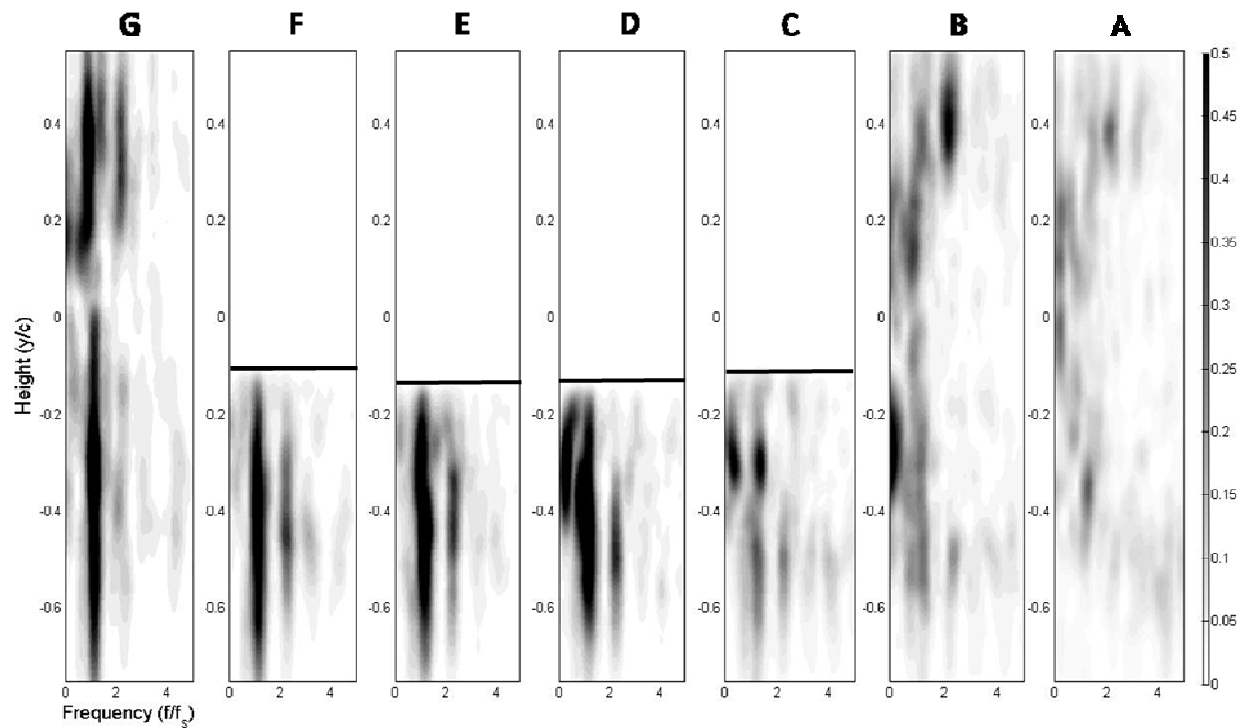


Figure 6. Spectral analysis of DPIV flow field at discrete slices. Note large energy at Strouhal frequency, indicating the circular cylinder has returned to its normal shedding frequency.

Wake organization was also seen in flow visualization experiments as shown in Figure 7 for  $M=0$  (left) and  $M=0.105$  (right) cases. These images were recorded in the second interrogation plane. The right snapshot very clearly shows the LEB/wake interaction which resulted in symmetric vortex street (five vortices are shown pointed with the arrows) situated

almost symmetrically about the airfoil centerline. The right picture appears to show symmetric (about the centerline of the airfoil) vortex production. The top and bottom vortices are skewed slightly, which could be attributed to the asymmetric location of the LEB jet about the airfoil.

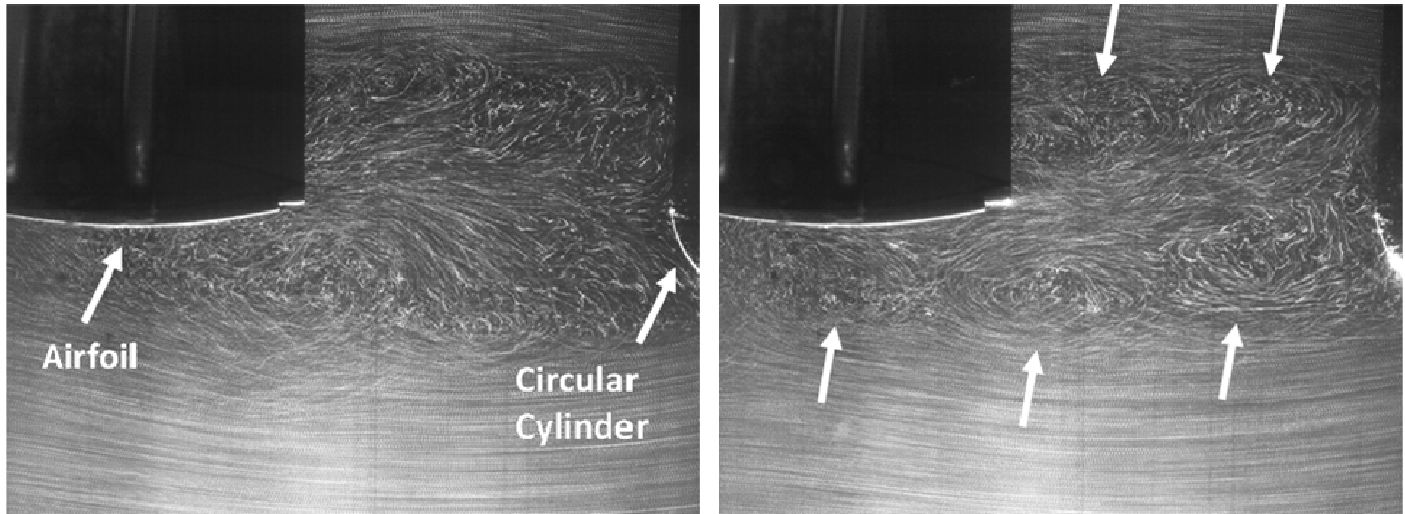


Figure 7. A flow visualization comparison between  $M=0$  (left) and  $M=0.105$  (right). The images are shown in interrogation plane 2. Note the presence of nearly symmetric vortices located top and bottom of the airfoil centerline.

### Discussion of the Proposed Wake Organization Mechanism

From the above analysis, it is evident that the wake has been organized with the application of the LEB jet and the wake recovers its normal vortex shedding frequency. Based on the available data, two mechanisms are proposed to account for the observed physics: A) penetration of the flow control jet onto the circular cylinder leeward side and B) interaction of the wake shear layers with the plane jet. In this fashion, the LEB jet acts to perturb the shear layers causing roll up and shed vortices. The data weakly supports mechanism A, and thus we focus mainly on proposed mechanism B.

It is well known that the airfoil (splitter plate) acts as an inhibitor of the cylinder shear layer communication, which apparently is a requirement for vortex shedding. Two hypotheses to explain the LEB induced shedding mechanism is that 1) the LEB jet restores the communication between the circular cylinder shear layers or 2) directly perturbs the shear layers causing instability. Both explanations largely center on the ability of the LEB jet to perturb the shear layers either indirectly (hypothesis 1) or directly (hypothesis 2). Other researchers have investigated the effects of perturbing the flow field so as to rearrange the wake structure. Konstantinidis et al [35] conducted water tunnel tests of a circular cylinder immersed in a freestream with a sinusoidal perturbation

velocity. They report bimodal behavior in the wake structure, namely switching between the 2S and 2P modes. Ongoren and Rockwell [36] studied the effects of oscillating the circular cylinder in the streamwise direction at very low oscillation amplitudes and reported a wake similar to the 2P mode. Thus evidence exists indicating a streamwise perturbation of the flow field can result in a mode similar to the 2P mode.

To understand the bulk effect of the LEB on the wake and shear layers, Figure 8 shows the mean wake velocity profiles for the no-blowing (left) and max-blowing (right) cases (every 10<sup>th</sup> vector shown for clarity). The velocity ratio magnitude is shown in grayscale, the shear layer being very clearly defined as the region of low velocity ratio magnitude. This Figure is largely responsible for disproving mechanism A as that responsible for the observed wake organization phenomenon. It is quite clear that the LEB jet does not have enough momentum to strike the leeward side of the circular cylinder. However, for larger blowing coefficients this mechanism could potentially affect the wake formation.

The shear layers are clearly modified by the LEB jet and act to push the shear layer impingement point on the airfoil further downstream. For no blowing the impingement point is  $x/c \sim -0.6$  while for max blowing the impingement point is  $x/c \sim -0.75$  (marked in the Figure as the dotted vertical lines). The curvature of the mean shear layer is modified as well, with no blowing the shear layer tends to curve towards the airfoil

further upstream ( $x/c \sim 0.45$ , region A) than with blowing ( $x/c \sim 0.1$ , region B). Thus it is clear that the jet modifies the mean

position of the shear layers.

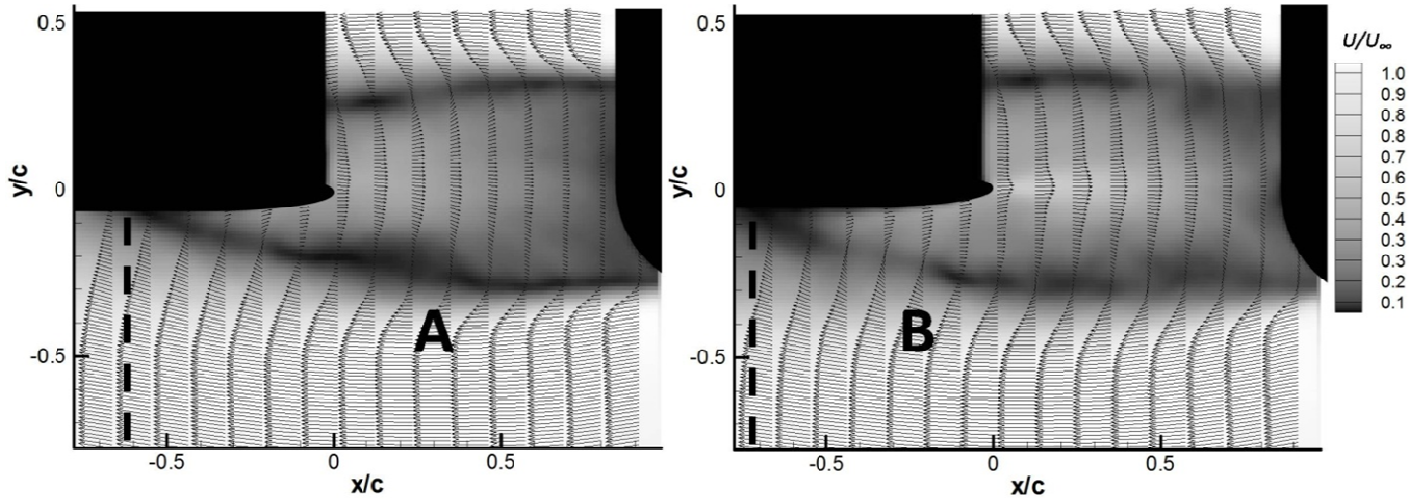


**Figure 8. Mean velocity profiles comparison between  $M=0$  (left) and  $M=0.105$  (right). The images are shown in interrogation plane 2. Note that with cross flow, the LEB jet does not appear to have enough momentum to strike the leeward side of the circular cylinder.**

The shear layer positions were directly tracked using the DPIV data to ascertain the effect of the LEB jet on their position and fluctuations. To perform the tracking, the central difference of the velocity field computed from 20 eigenmodes was computed at every  $x/c$  slice (i.e. a 1D derivative computed at multiple  $x/c$  locations). The result was median filtered on a grid of  $5 \times 5$  pixels and the local maxima and minima were computed to locate the shear layers. Figure 9 shows the computed standard deviation of the shear layer position for each blowing case. A comparison of the upper and lower shear layers with and without blowing reveals an increased level of shear layer activity with blowing, thus indicating that the shear layers themselves are affected by the LEB. Additionally, note that the shear layer excitation increases, in particular for the max blowing case, as the shear layers approach the LEB slot, located at  $x/c=0$ .

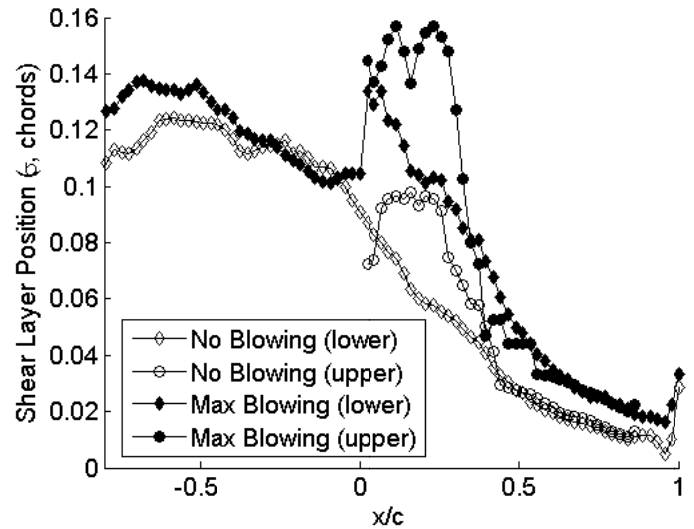


**Figure 9. The shear layers were located using central difference derivative approximations of the velocity field at every  $x/c$  slice. The standard deviation of the shear layer position was calculated to observe the change in shear layer character. Note the large increase as the shear layer approaches the leading edge, and blowing slot, of the airfoil.**

To understand how the near wake velocity measurements behave as a system, Figure 10 shows the results of a cross correlation computed between the  $u'$  velocity series at one point ( $x/c=0.4$ ,  $y/c=-0.2$ ; denoted as intersection of dotted lines) with every other point in the flow field for both  $M=0$  and  $M=0.105$  in interrogation plane two. The streamwise perturbations were chosen for this argument because evidence exists to suggest that streamwise perturbations can result in 2P shedding modes



([35]; [36]). Only the maximum correlation magnitude is shown (lag information is shown in Figure 11). The fixed (base) correlation point is seen in both cases as the overpowering black region since this forms the autocorrelation of the signal and thus its magnitude is greatest. For  $M=0$  mild correlation is seen between the upper and lower circular cylinder shear layers with relatively no correlation in the spatial region between the two, corroborating the idea that the upper

and lower shear layers are acting independently as is expected with a splitter plate present. This is denoted by the region  $-0.2 < y/c < 0.2$  having a small ( $< 0.15$ ) correlation magnitude. This represents a relatively uncorrelated wake. This point also correlates, to a lesser extent, with the outer flow. For  $M=0.105$ , the base point has essentially no correlation whatsoever with the outer flow but excellent correlation is seen throughout the circular cylinder wake.

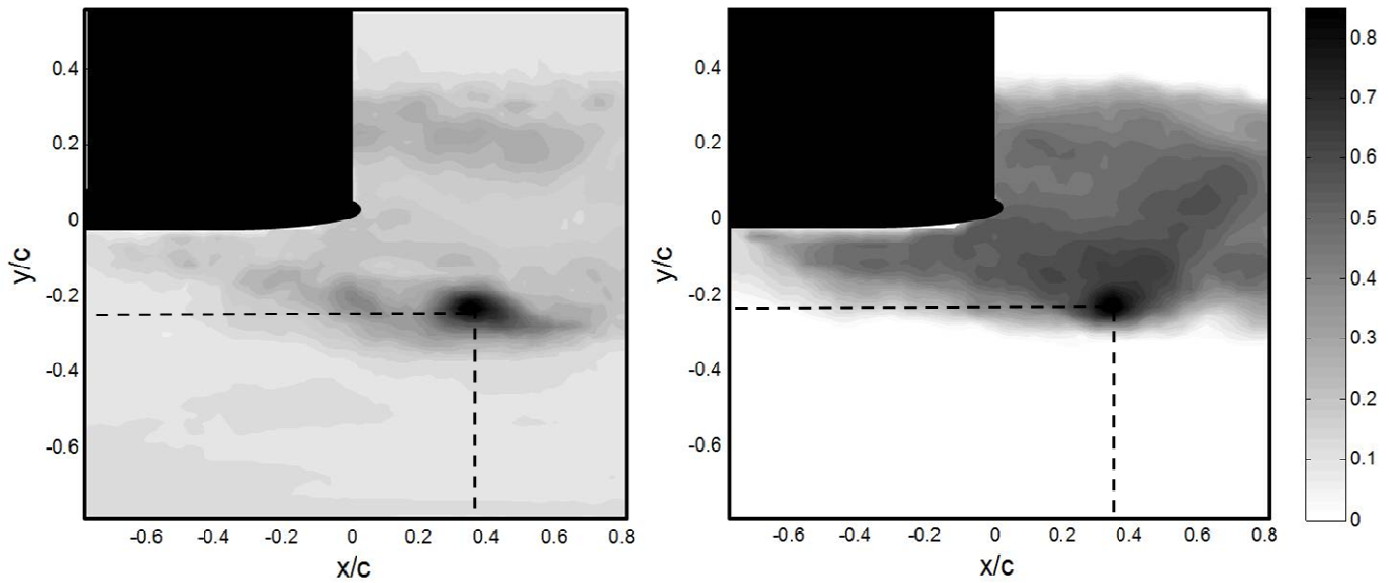


**Figure 10. Cross correlation of a single point on the circular cylinder shear layer with all other points in the velocity field. Results are shown in interrogation plane two for  $M=0$  (left) and  $M=0.105$  (right).**

From Figure 10 it is clear that the LEB acts to organize the wake as it is highly correlated with the application of the LEB jet. Examination of the lag information contained in the cross correlations are shown at discrete slices of  $x/c$  in Figure 11 to determine the phase of the maximum correlation magnitudes shown in Figure 10. The approximate wake width is denoted by the black lines. With the application of LEB the  $u'$  velocity throughout the wake ( $-0.2 < y/c < 0.2$ ) becomes in phase (i.e. zero lag). The situation is quite reversed for  $M=0$ , although along the circular cylinder shear layers there are regions of high correlation, being both in and out of phase. However since the cross correlations are taken with respect to one fixed point it is not certain whether or not the shear layers are just physically similar or necessarily communicative. Note that in the areas immediately outside of the circular cylinder shear layer ( $y/c > 0.2$  and  $y/c < -0.2$ ) the oscillations become out of phase.

It is well known that plane jets flap in a direction normal to the spanwise plane and it has been theorized that it is the coherent structures inherent in the plane jet which are responsible for this phenomenon ([22]; [23]). From the correlation and phase information shown in Figure 10 and

Figure 11 it is hypothesized that the LEB jet coupled with the upper and lower circular cylinder shear layers form a system which oscillates together. That is, the jet perturbs the shear layers which in turn shed at a distinct frequency, thus perturbing the jet and resulting in a phase locking phenomenon. This hypothesis explains both the increased wake correlation and the zero phase lag with the LEB jet applied, as well as the observation of increased wake coherency. The hypothesized system thus resembles that typically seen with a circular cylinder free to oscillate in a uniform freestream in the vertical direction only instead of the circular cylinder oscillating to couple with the wake, the jet performs this role.

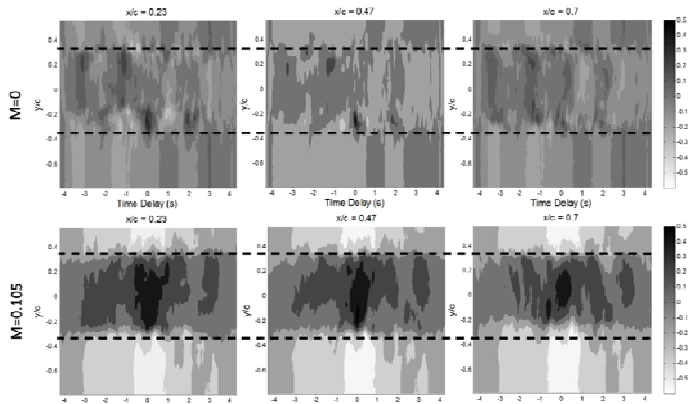


**Figure 11. Cross correlation details for several  $x/c$  slices with approximate wake width shown by dotted black lines. Results are shown for interrogation plane two for  $M=0$  (top row) and  $M=0.105$  (bottom row). Note that the LEB acts to bring the near wake region into phase, indicating a possible phase lock mechanism.**

## CONCLUSIONS AND FUTURE WORK

Time Resolved Digital Particle Image Velocimetry (TRDPIV) was used in conjunction with spectral analysis and the Proper Orthogonal Decomposition (POD) to study the effects of Leading Edge Blowing (LEB) flow control on the near-wake of a circular cylinder and the Blade Vortex Interaction (BVI) arising from the wake and an airfoil. Results indicated that for no flow control the airfoil acted as a splitter plate as anticipated. Spectral measurements of the TRDPIV results indicated that the plate decreased the Strouhal number from 0.19 to 0.12. This is similar to the results reported by Ozono [34], who showed in his experiments that a splitter plate 2 diameters downstream of a circular cylinder yields a Strouhal number of 0.13.

The LEB jet was shown to organize the wake, effectively neutralizing the effect of the splitter plate and modifying the wake so as to return the Strouhal number to 0.19. Evidence exists to support the concept that the LEB jet perturbs the shear layers directly, perhaps through the familiar flapping often observed in plane jets. This may be due to a phase locking mechanism, coupling the shear layer shedding and plane jet flapping motions. Specifically, this hypothesis is supported by four observations of the data:

1. It does not appear that the LEB jet has enough momentum in the presence of the cross flow to pierce the wake and strike the leeward side of the circular cylinder. Thus the LEB jet does not appear to disrupt the shear layer development near the circular cylinder.
2. It was shown that the mean positions of the shear layers are affected by the LEB jet (Figure 8). Additionally, trends in the excitation of the shear layers were shown to exhibit greater fluctuations with LEB applied with the greatest level of excitation close to the airfoil blowing slot (Figure 9).

3. The velocity fluctuations in the near wake become greatly correlated with the application of LEB (Figure 10). Particularly interesting is that the velocity fluctuations in the near wake become have zero phase lag with the LEB applied (Figure 11). It appears that the near wake was modified into a coherent system which resulted in vortex shedding similar to a 2P mode at the normal Strouhal frequency.

## ACKNOWLEDGMENTS

This research was sponsored by Techsburg, Inc through ONR contract number N00014-03-M-0277. The authors also wish to acknowledge the help of Patrick Leung in taking the initial TRDPIV data.

## REFERENCES

- [1] Rockwell, D., 1998, "Vortex-Body Interactions," Annual Review of Fluid Mechanics, 30(pp. 30).
- [2] Williamson, C., and Govardhan, R., 2004, "Vortex-Induced Vibrations," Annual Review of Fluid Mechanics, 36(pp. 42).
- [3] Hardin, J., and Lamkin, S., 1986, "Concepts for Reduction of Blade-Vortex Interaction Noise.," Journal of Aircraft, 24(pp. 5).
- [4] Jadic, I., So, R., and Mignolet, M., 1998, "Analysis of Fluid-Structure Interactions Using a Time-Marching Technique," Journal of Fluids and Structures, 12(pp. 23).
- [5] Johnston, R., and Fleeter, S., 2001, "Inlet Guide Vane Wakes Including Rotor Effects," Journal of Fluids and Structures, 15(pp. 18).
- [6] Yu, Y., 1996,
- [7] Coton, F., Green, R., Early, J., and Price, J., 2005,
- [8] Lee, S., 1994, "Reduction of Blade-Vortex Interaction Noise through Porous Leading Edge," AIAA Journal, 32(pp. 8).
- [9] Weiland, C., and Vlachos, P., 2009, "A Mechanism for Mitigation of Blade Vortex Interaction Using Leading Edge Blowing Flow Control," Experiments in Fluids, 47(3), pp. 15.
- [10] Mansingh, V., and Oosthuizen, P., 1989, "Effects of Splitter Plates on the Wake Flow Behind a Bluff Body," AIAA Journal, 28(pp. 6).
- [11] Anderson, E., and Szweczyk, A., 1997, "Effects of a Splitter Plate on the near Wake of a Circular Cylinder in 2 and 3-Dimensional Flow Configurations," Experiments in Fluids, 23(pp. 13).
- [12] You, D., Haecheon, C., Choi, M., and Kang, S., 1998, "Control of Flow-Induced Noise Behind a Circular Cylinder Using Splitter Plates," AIAA Journal, 36(pp. 6).
- [13] Bull, M., Blazewicz, A., Pickles, J., and Bies, D., 1996, "Interaction between a Vortex Wake and an Immersed Rectangular Plate," Experimental Thermal and Fluid Science, 12(pp. 11).
- [14] Williamson, C., 1996, "Vortex Dynamics in the Cylinder Wake," Annual Review of Fluid Mechanics, 28(pp. 62).

- [15] Huerre, P., and Monkewitz, P., 1990, "Local and Global Instabilities in Spatially Developing Flows," *Annual Review of Fluid Mechanics*, 22(pp. 64.
- [16] Lin, J., Towfighi, J., and Rockwell, D., 1995, "Instantaneous Structure of the near-Wake of a Circular Cylinder: On the Effect of Reynolds Number," *Journal of Fluids and Structures*, 9(pp. 9.
- [17] Unal, M., and Rockwell, D., 1987, "On Vortex Formation from a Cylinder. Part 1. The Initial Instability.," *Journal of Fluid Mechanics*, 190(pp. 21.
- [18] Grove, A., Shair, F., Peterson, E., and Acrivos, A., 1964, "An Experimental Investigation of the Steady Separated Flow Past a Circular Cylinder," *Journal of Fluid Mechanics*, 19(pp. 20.
- [19] Unal, M., and Rockwell, D., 1987, "On Vortex Formation from a Cylinder. Part 2. Control by Splitter-Plate Interference.," *Journal of Fluid Mechanics*, 190(pp. 16.
- [20] Ziada, S., and Rockwell, D., 1982, "Vortex-Leading-Edge Interaction," *Journal of Fluid Mechanics*, 118(pp. 28.
- [21] Lin, J., and Rockwell, D., 2001, "Oscillations of a Turbulent Jet Incident Upon an Edge," *Journal of Fluids and Structures*, 15(pp. 38.
- [22] Gordeyev, S., and Thomas, F., 2000, "Coherent Structure in the Turbulent Planar Jet. Part 2. Structural Topology Via Pod Eigenmode Projection," *Journal of Fluid Mechanics*, 414(pp. 49.
- [23] Antonia, R., Browne, L., Rajagopalan, S., and Chambers, A., 1983, "On the Organized Motion of a Turbulent Plane Jet," *Journal of Fluid Mechanics*, 134(pp. 17.
- [24] Gordeyev, S., and Thomas, F., 2002, "Coherent Structure in the Turbulent Planar Jet. Part 1. Extraction of Proper Orthogonal Decomposition Eigenmodes and Their Self-Similarity.," *Journal of Fluid Mechanics*, 460(pp. 31.
- [25] Hsiao, F., Chou, Y., and Huang, J., 1999, "The Study of Self-Sustained Oscillating Plane Jet Flow Impinging Upon a Small Cylinder," *Experiments in Fluids*, 27(pp. 7.
- [26] Hsiao, F., Hsu, I., and Huang, J., 2004, "Evolution of Coherent Structures and Feedback Mechanism of the Plane Jet Impinging on a Small Cylinder," *Journal of Sound and Vibration*, 278(pp. 16.
- [27] Popiel, C., and Trass, O., 1991, "Visualization of a Free and Impinging Round Jet," *Experimental Thermal and Fluid Science*, 4(pp. 11.
- [28] Cornaro, C., Fleischer, A., and Goldstein, A., 1999, "Flow Visualization of a Round Jet Impinging on Cylindrical Surfaces," *Experimental Thermal and Fluid Science*, 20(pp. 12.
- [29] Fleischer, A., Kramer, K., and Goldstein, R., 2001, "Dynamics of the Vortex Structure of a Jet Impinging on a Convex Surface," *Experimental Thermal and Fluid Science*, 24(pp. 6.
- [30] Fey, U., Koenig, M., and Eckelmann, H., 1998, "A New Strouhal-Reynolds-Number Relationship for the Circular Cylinder in the Range  $47 < Re < 2 \times 10^5$ ," *Physics of Fluids*, 10(pp. 2.
- [31] Adrian, R., 2005, "Twenty Years of Particle Image Velocimetry," *Experiments in Fluids*, 39(pp. 10.
- [32] Willet, C., and Gharib, M., 1991, "Digital Particle Image Velocimetry," *Experiments in Fluids*, 10(pp. 12.
- [33] Abiven, C., and Vlachos, P., 2002,
- [34] Ozono, S., 1999, "Flow Control of Vortex Shedding by a Short Splitter Plate Asymmetrically Arranged Downstream of a Cylinder," *Physics of Fluids*, 11(pp. 6.
- [35] Konstantinidis, E., Balabani, S., and Yianneskis, M., 2007, "Bimodal Vortex Shedding in a Perturbed Cylinder Wake," *Physics of Fluids*, 19(pp.
- [36] Ongoren, A., and Rockwell, D., 1988, "Flow Structure from an Oscillating Cylinder Part 2. Mode Competition in the near Wake.," *Journal of Fluid Mechanics*, 191(pp. 20.